THE JOURNAL OF PHYSICAL CHEMISTRY B

Article

pubs.acs.org/JPCB

An Equilibrium Model for Chiral Amplification in Supramolecular Polymers

Huub M. M. ten Eikelder,*[,†,§] Albert J. Markvoort,[†,§] Tom F. A. de Greef,[†,‡,§] and Peter A. J. Hilbers[†,§]

[†]Institute for Complex Molecular Systems, [‡]Laboratory for Macromolecular and Organic Chemistry, and [§]Biomodeling and Bioinformatics Group, Eindhoven University of Technology, Eindhoven, The Netherlands

Supporting Information

ABSTRACT: We describe a model that rationalizes amplification of chirality in cooperative supramolecular copolymerization. The model extends nucleation-elongation based equilibrium models for growth of supramolecular homopolymers to the case of two monomer and aggregate types. Using the principle of mass-balance for the two monomer types, we derive a set of two nonlinear equations, describing the thermodynamic equilibrium state of the system. These equations can be solved by numerical methods, but also analytical approximations are derived. The equilibrium model allows two-sided growth of the aggregates and can be applied to symmetric supramolecular copolymerizations, corresponding to the situation in which the monomers are enantiomerically related, as well as to the more general case of nonsymmetric supramolecular copolymerizations. In detail, so-called majority-rules phenomena in supramolecular systems with isodesmic as well as cooperative growth are analyzed. Comparison of model predictions with experimental data shows that the model gives a very good description of both titration and melting curves. When the system shows cooperative growth, the model leads to a phase diagram in which the presence of the various aggregate types is given as a function of composition and temperature.

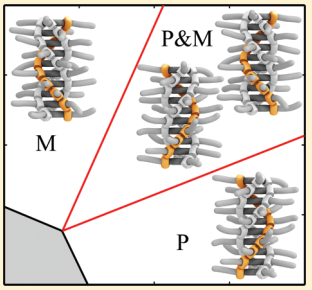

1. INTRODUCTION

Self-assembly of molecules into large clusters is a general phenomenon in chemistry, physics, and biology. When the interaction between the monomers is generated by moderately strong, reversible noncovalent, but highly directional, forces that result in high molecular weight linear aggregates under dilute conditions, the self-assembly is classified as a supramolecular polymerization.[1] Various molecules, ranging from aromatic molecules such as larger hexabenzocoronenes[2] and phenylacetylene macrocycles,[3] to complete proteins like β_2-microglobulin,[4] are known to self-assemble into filamentary aggregates, in which the intermolecular interactions can range from $\pi-\pi$ interactions to hydrogen bonding and Coulombic interactions.

The formation of such supramolecular polymers has been studied both experimentally and theoretically. The case where the aggregates are formed from a single component is well understood. Several models exist to describe the thermodynamic equilibrium state[5−11] as well as their kinetics.[12−15] The most simple set of reactions to describe the formation of dynamic supramolecular polymers from a single type of monomers is given by

$$\mathrm{X} + \mathrm{X} \underset{c_{-2}}{\overset{c_2}{\rightleftharpoons}} \mathrm{X}_2 \tag{1}$$

$$\mathrm{X}_{i-1} + \mathrm{X} \underset{c_{-i}}{\overset{c_i}{\rightleftharpoons}} \mathrm{X}_i \quad (i > 2) \tag{2}$$

where X represents the monomer, X_2 is the dimer, and X_i is the oligomer/polymer of length i. The first reaction describes the equilibrium between monomers and dimers and the second reaction describes additions and removals to/from existing oligomers and aggregates.

In principle, all rate constants could be specified individually, but usually some assumptions are made. In the simplest model, that is, the isodesmic model,[5] it is assumed that the equilibrium constants for all monomer additions to another monomer or to a supramolecular polymer are equal, that is, all equilibrium constants $K_i = c_i/c_{-i}$ are equal to a constant K. This isodesmic model can be extended in two ways to describe cooperative supramolecular polymerizations. In the nucleation−elongation models,[6,7] the equilibrium constants are different for monomer additions before the supramolecular polymer has reached a critical nucleus size n and monomer additions to supramolecular polymers with a length at least n. The second approach is to describe the cooperative supramolecular polymerization as a thermally activated equilibrium supramolecular polymerization.[8,9] In this type of supramolecular polymerization there is an additional reaction between active and inactive monomers, and only the active monomers are able to form new dimers. The thermally activated equilibrium model has been extended, using a so-called helix-reversal-penalty, to describe also the supramolecular copolymerization of two enantiomers, which has been used to model chiral amplification in supramolecular polymerization of benzene-1,3,5-tricarboxamides (BTAs).[16−18]

Received: January 18, 2012
Revised: March 21, 2012
Published: March 23, 2012

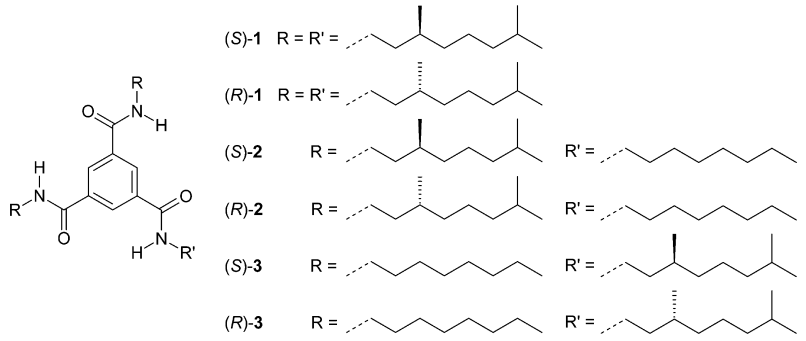

Figure 1. Molecular structure[16,17] of the different symmetrically and asymmetrically substituted benzene-1,3,5-tricarboxamides used in this study.

Here we extend the nucleation−elongation model to two component systems (monomers R and S) that can form two types of supramolecular polymers, for example, aggregates with two types of helicity (P and M), such that it can be used to model chiral amplification in supramolecular copolymerization as well. In particular, we will focus on the so-called majority-rules phenomena,[19] where in the supramolecular copolymerization of two enantiomers a slight excess of one enantiomer leads to a strong bias toward aggregates with the helicity corresponding to the major enantiomer. In our model the equilibrium state is found as the solution of the *mass-balance equations*. An earlier version of the mass-balance model has been described in ref 21. In the current paper we give a more detailed derivation of the mass-balance equations and extend the model to allow two-sided growth of the supramolecular polymers, which is chemically more realistic. Moreover, we also consider the case of nonsymmetric supramolecular copolymerization, for instance if the monomers are not enantiomerically related. We verify the results of our model with experimental titration curves and melting curves of symmetrically and nonsymmetrically substituted benzene-1,3,5-tricarboxamides (see Figure 1) that are known to form helical supramolecular polymers via 3-fold hydrogen bonding. As an example in which aggregation occurs via an isodesmic growth mechanism, the supramolecular copolymerization of 3,3′-diamino-2,2′-bipyridine C3-discotics (*S*)-**4** and (*R*)-**4**[20] (see Figure 2) will be analyzed. In all cases, a very good description of the experimental results is obtained.

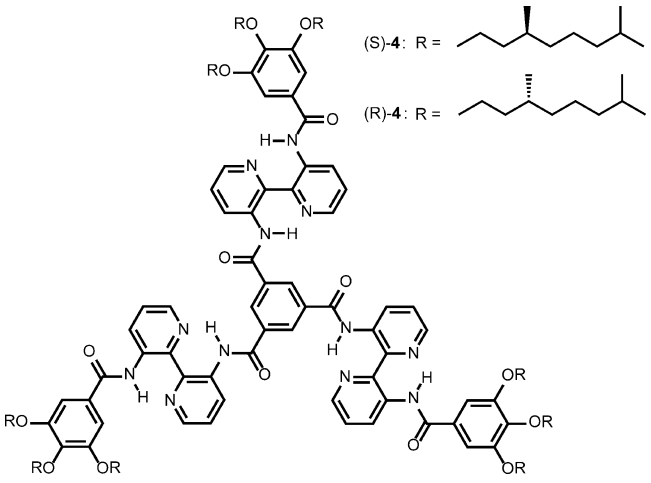

Figure 2. Molecular structure[20] of the C3-symmetrical disk-shaped compounds (*S*)-**4** and (*R*)-**4**.

Moreover, the model allows to compute a phase diagram that describes the presence of P-type and/or M-type aggregates in solution as a function of the total concentration of R monomers, r_{tot}, the total concentration of S monomers, s_{tot}, and the temperature, T. Four regions are discerned, that is, monomers and both supramolecular polymer types (I), monomers and P-type supramolecular polymers (IIa), monomers and M-type supramolecular polymers (IIb), and only monomers (III). The boundaries between the various regions in the phase diagram are described using a critical value of the enantiomeric excess and elongation temperatures for P-type and for M-type supramolecular polymers.

In the next section, we derive the mass-balance model describing the thermodynamic equilibrium of a two-component, two-aggregates type system. In section 3, the properties of the mass-balance equations will be studied in detail. We give a numerical solution, an analytical approximation to that solution, and we study the phase space of the system. The model results are compared with experimental data in section 4. Some concluding remarks are made in section 5. Moreover, in the Supporting Information, software is supplied that allows to obtain the thermodynamical parameters of the model by nonlinear least-squares fitting of the model results to experimental data.

2. MASS-BALANCE MODEL

First we describe the chemical reactions that model the formation of supramolecular polymers from two distinct components (R and S) that can aggregate into two different types of supramolecular polymers (either P- or M-type helicity). Both P- and M-type aggregates will be written as a sequence of R and S molecules, with the left molecule representing the bottom of the aggregate and the right molecule representing the top of the aggregate. To indicate whether the sequence represents a P- or M-type supramolecular polymer, the superscripts (P) or (M) are used. Hence, $RRSR^{(P)}$ represents a P-type aggregate of length 4 and $SRSSS^{(M)}$ represents an M-type aggregate of length 5, and $RSRR^{(P)}$ is a different aggregate than its reverse $RRSR^{(P)}$.

Formation of P-type supramolecular polymers. We first describe the formation of P-type aggregates in more detail. Growth of the supramolecular polymers is assumed to occur via a nucleation-elongation growth mechanism with nucleus size $n = 2$. During nucleation, formation of P dimers is described by the following reactions

$$R + R \underset{\hat{k}_{-1}}{\overset{\hat{k}_1}{\rightleftharpoons}} RR^{(P)} \tag{3}$$

dx.doi.org/10.1021/jp300622m | J. Phys. Chem. B 2012, 116, 5291−5301

$$R + S \underset{\hat{k}_{-2}}{\overset{\hat{k}_2}{\rightleftharpoons}} RS^{(P)} \tag{4}$$

$$R + S \underset{\hat{k}_{-2}}{\overset{\hat{k}_2}{\rightleftharpoons}} SR^{(P)} \tag{5}$$

$$S + S \underset{\hat{k}_{-3}}{\overset{\hat{k}_3}{\rightleftharpoons}} SS^{(P)} \tag{6}$$

in which we assumed that the rate constants to form $RS^{(P)}$ and $SR^{(P)}$ are equal. The corresponding equilibrium constants are given by $\hat{K}_1 = \hat{k}_1/\hat{k}_{-1}$, $\hat{K}_2 = \hat{k}_2/\hat{k}_{-2}$ and $\hat{K}_3 = \hat{k}_3/\hat{k}_{-3}$. In the elongation regime longer P-type aggregates are formed by addition of an R or S molecule at the top or bottom of an existing P-type aggregate. Using P_l for an arbitrary P-type supramolecular polymer of length $l \geq 2$, we assume that elongation is described by

$$P_l + R \underset{k_{-1}}{\overset{k_1}{\rightleftharpoons}} P_lR \tag{7}$$

$$P_l + R \underset{k_{-1}}{\overset{k_1}{\rightleftharpoons}} RP_l \tag{8}$$

$$P_l + S \underset{k_{-2}}{\overset{k_2}{\rightleftharpoons}} P_lS \tag{9}$$

$$P_l + S \underset{k_{-2}}{\overset{k_2}{\rightleftharpoons}} SP_l \tag{10}$$

Note that the addition of an R monomer to the bottom or top of a P-type aggregate has the same reaction constants for all P-type aggregates. The same holds for the addition of an S monomer to the bottom or top of a P-type aggregate. However, the addition of an R monomer to a P-type aggregate will, in general, be different from the addition of an S monomer. The equilibrium constants in the elongation regime, which are thus independent of the aggregate length l, will be denoted as $K_1 = k_1/k_{-1}$ and $K_2 = k_2/k_{-2}$.

Two-Sided Growth and Detailed Balance. The *principle of detailed balance* states that in thermodynamic equilibrium for each individual reversible reaction the forward and backward fluxes are equal. Square bracket notation will be used to indicate the equilibrium concentration of a molecule type, that is, $[RS^{(P)}]$ denotes the equilibrium concentration of RS dimers with P-type helicity. Moreover, we shall use the abbreviations

$$r = [R]$$

and

$$s = [S]$$

for the free monomer concentrations in the equilibrium state. For the reaction in eq 4, the principle of detailed balance implies that in equilibrium $[RS]^{(P)} = \hat{K}_2 rs$. The combination of the principle of detailed balance with two-sided aggregate growth implies that not all equilibrium constants are independent. For example, the trimer $RRS^{(P)}$ can be produced by addition of an R molecule at the bottom of the dimer $RS^{(P)}$, yielding $[RRS^{(P)}] = K_1 r[RS^{(P)}] = K_1\hat{K}_2 r^2 s$. However, $RRS^{(P)}$ can also be produced by addition an S monomer at the top of the $RR^{(P)}$ dimer, leading to $[RRS^{(P)}] = K_2 s[RR^{(P)}] = K_2\hat{K}_1 r^2 s$. Hence, the equilibrium constants must be related by $K_1\hat{K}_2 = K_2\hat{K}_1$. Consequently, we can introduce the cooperativity factor for P-type supramolecular polymers σ_P by

$$\sigma_P = \frac{\hat{K}_1}{K_1} = \frac{\hat{K}_2}{K_2} \tag{11}$$

In a similar way it can be shown that $\hat{K}_3$ cannot be chosen independently. Formation of trimer $SSR^{(P)}$ by addition of an R monomer at the top of an $SS^{(P)}$ dimer results in $[SSR^{(P)}] = K_1 r[SS^{(P)}] = K_1\hat{K}_3 rs^2$, while addition of an S monomer at the bottom of an $SR^{(P)}$ dimer leads to $[SSR^{(P)}] = K_2 s[SR^{(P)}] = K_2\hat{K}_2 rs^2$. Hence, we conclude that equilibrium constant $\hat{K}_3$ can be written as

$$\hat{K}_3 = \frac{K_2\hat{K}_2}{K_1} \tag{12}$$

Note that eqs 11 and 12 imply that the various equilibrium constants for the formation of P-type supramolecular polymers are all determined by the values of K_1, K_2, and σ_P. In fact, the mutual dependence of the various equilibrium constants is a consequence of detailed balance and the presence of cycles in the system of reactions.[22−24]

Concentrations of Various Supramolecular Polymer Types. The principle of detailed balance also implies that the concentration of every kind of P-type or M-type aggregate can be expressed in terms of the monomer concentrations r and s. The concentration of a P-type aggregates depends only on the number of R and S monomers present in the aggregate, not on their positions. If we define $p_{i,j}$ as the concentration of an arbitrary P-type supramolecular polymer that contains i molecules R and j molecules S, then

$$p_{i,j} = \frac{\sigma_P}{K_1}(K_1 r)^i (K_2 s)^j \tag{13}$$

It is easily verified that eq 13 holds for all four dimer types. Moreover, eq 13 also holds for longer aggregates because the addition of an R or S monomer to a P-type aggregate means that the concentration must be multiplied by $K_1 r$ or $K_2 s$, respectively.

Next we turn to the total amount of R and S molecules present in P-type supramolecular polymers of length l. A P-type supramolecular polymer of length l can contain $i = 0, 1, ..., l$ molecules R and, hence, $j = l - i$ molecules S. Each selection of i positions (for the R molecules) out of the total of l positions gives a different aggregate type. Hence the total number of different P-type supramolecular polymers of length l with i molecules R (and $l - i$ molecules S) is given by the binomial coefficient $\binom{l}{i}$. For instance, there are $\binom{4}{2} = 6$ different types of P-type aggregates with length 4 and 2 R molecules, namely, $RRSS^{(P)}$, $RSRS^{(P)}$, $RSSR^{(P)}$, $SRRS^{(P)}$, $SRSR^{(P)}$, and $SSRR^{(P)}$. Let r_{P_l} be the concentration of R molecules in P-type supramolecular polymers of length l. More precisely, if all R molecules in these P-type aggregates would be "free monomers", these monomers have a concentration r_{P_l}. Since $p_{i,j}$ is the concentration of an arbitrary P-type aggregate with i molecules R and j molecules

dx.doi.org/10.1021/jp300622m | J. Phys. Chem. B 2012, 116, 5291−5301

S, and there are $\binom{l}{i}$ different aggregates of this type, we conclude that

$$r_{P_l} = \sum_{i=0}^{l} \binom{l}{i} i p_{i,l-i}$$

With some algebra (see Supporting Information, section SI-1), this term can be rewritten as

$$r_{P_l} = \sigma_P r l g_p^{l-1}$$

where the *elongation factor* for P-type supramolecular polymers is defined as

$$g_p \equiv K_1 r + K_2 s$$

Similarly, we define s_{P_l} as the concentration of S monomers that correspond to all S molecules in P-type aggregates of length l. Then a similar computation yields

$$s_{P_l} = \sum_{i=0}^{l} \binom{l}{i} (l-i) p_{i,l-i} = \frac{K_2}{K_1} \sigma_P s l g_p^{l-1}$$

Note that the elongation factor $g_p < 1$, otherwise, the total amount of S and R molecules in P-type aggregates of length l, would increase as function of l, which means that concentration of all P-type aggregates would be infinite.

The fraction of R molecules in P-type supramolecular polymers of length l is now found to be

$$\frac{r_{P_l}}{r_{P_l} + s_{P_l}} = \frac{K_1 r}{K_1 r + K_2 s}$$

which is independent of the length of the aggregate.

Knowing the amount R and S molecules in P-type aggregates of length l, it is now possible to compute the amount of R and S molecules in all P-type aggregates. Let r_P be the concentration of R molecules in all P-type supramolecular polymers. More precisely, if the R molecules in all P-type supramolecular polymers would be "free monomers", these monomers have a concentration r_P. Then

$$r_P = \sum_{l=2}^{\infty} r_{P_l} = \sigma_P r \sum_{l=2}^{\infty} l g_p^{l-1} = \sigma_P r \frac{g_p(2-g_p)}{(1-g_p)^2} \tag{14}$$

For details of the last step, see Supporting Information, section SI-1. Similarly, if s_P denotes the concentration of all S molecules that occur in P-type aggregates, then we obtain

$$s_P = \sum_{l=2}^{\infty} s_{P_l} = \frac{K_2}{K_1} \sigma_P s \sum_{l=2}^{\infty} l g_p^{l-1} = \frac{K_2}{K_1} \sigma_P s \frac{g_p(2-g_p)}{(1-g_p)^2} \tag{15}$$

Formation of M-Type Supramolecular Polymers. M-type aggregates also consist of R and S monomers, but in the formation of M-type aggregates, the role of R and S monomers will be interchanged compared to the formation of P-type supramolecular polymers. The nucleation regime, that is, the formation of M-type dimers, is governed by reactions

$$S + S \underset{\hat{k}_{-4}}{\overset{\hat{k}_4}{\rightleftharpoons}} SS^{(M)} \tag{16}$$

$$S + R \underset{\hat{k}_{-5}}{\overset{\hat{k}_5}{\rightleftharpoons}} SR^{(M)} \tag{17}$$

$$S + R \underset{\hat{k}_{-5}}{\overset{\hat{k}_5}{\rightleftharpoons}} RS^{(M)} \tag{18}$$

$$R + R \underset{\hat{k}_{-6}}{\overset{\hat{k}_6}{\rightleftharpoons}} RR^{(M)} \tag{19}$$

with corresponding equilibrium constants given by $\hat{K}_4 = \hat{k}_4/\hat{k}_{-4}$, $\hat{K}_5 = \hat{k}_5/\hat{k}_{-5}$, and $\hat{K}_6 = \hat{k}_6/\hat{k}_{-6}$. In the elongation regime, longer M-type aggregates are formed by addition of an S or R monomer at the top or bottom of an existing M-type aggregate. If M_l represents an arbitrary M-type aggregate of length $l \geq 2$, elongation is described by

$$M_l + S \underset{k_{-4}}{\overset{k_4}{\rightleftharpoons}} M_l S \tag{20}$$

$$M_l + S \underset{k_{-4}}{\overset{k_4}{\rightleftharpoons}} S M_l \tag{21}$$

$$M_l + R \underset{k_{-5}}{\overset{k_5}{\rightleftharpoons}} M_l R \tag{22}$$

$$M_l + R \underset{k_{-5}}{\overset{k_5}{\rightleftharpoons}} R M_l \tag{23}$$

with equilibrium constants $K_4 = k_4/k_{-4}$ and $K_5 = k_5/k_{-5}$.

The analysis of M-type aggregates is completely analogous to the analysis of P-type supramolecular polymers, as given in the previous subsection, and only the final results are given. The detailed balance condition now implies that $K_4\hat{K}_5 = \hat{K}_4 K_5$, which means we can define the cooperativity factor for M-type supramolecular polymers σ_M by

$$\sigma_M = \frac{\hat{K}_4}{K_4} = \frac{\hat{K}_5}{K_5} \tag{24}$$

Also, the equilibrium constant $\hat{K}_6$ is related to the other constants by

$$\hat{K}_6 = \frac{K_5 \hat{K}_5}{K_4} \tag{25}$$

Equation 25 means that the various equilibrium constants for the formation of M-type aggregates are all determined by the values of K_4, K_5, and σ_M. If we define s_M and r_M as the concentrations of S and R monomers that occur in M-type supramolecular polymers, respectively, then a similar computation as in the previous section results in

$$s_M = \sigma_M s \frac{g_m(2-g_m)}{(1-g_m)^2} \tag{26}$$

$$r_M = \frac{K_5}{K_4} \sigma_M r \frac{g_m(2-g_m)}{(1-g_m)^2} \tag{27}$$

where g_m is the elongation factor for M-type supramolecular polymers, defined by

$$g_m \equiv K_4 s + K_5 r$$

Also, g_m must be smaller than 1 to keep the system finite.

dx.doi.org/10.1021/jp300622m | J. Phys. Chem. B 2012, 116, 5291−5301

Mass-Balance Equations. So far we have expressed the concentrations of R and S molecules occurring in P-type and M-type aggregates in terms of the free monomer concentrations r and s. However, these monomer concentrations are still unknown. Next we show how r and s can be computed.

Suppose the total number of R molecules present in the system corresponds to a concentration r_{tot}. Each R molecule is either a monomer, part of a P-type aggregate, or part of an M-type aggregate. Hence, mass conservation for R molecules means that $r + r_P + r_M = r_{tot}$. Using eqs 14 and 27, this yields

$$r + \sigma_P r \frac{g_p(2 - g_p)}{(1 - g_p)^2} + \frac{K_5}{K_4}\sigma_M r \frac{g_m(2 - g_m)}{(1 - g_m)^2} = r_{tot} \tag{28}$$

Similarly, each S molecule is either a monomer, part of a P-type aggregate, or part of an M-type aggregate. Hence, $s + s_p + s_M = s_{tot}$, where s_{tot} is the total concentration of S molecules in the system. Using eqs 15 and 26, this yields

$$s + \sigma_M s \frac{g_m(2 - g_m)}{(1 - g_m)^2} + \frac{K_2}{K_1}\sigma_P s \frac{g_p(2 - g_p)}{(1 - g_p)^2} = s_{tot} \tag{29}$$

Equations 28 and 29 are the mass-balance equations, which form two (nonlinear) equations with r and s as unknowns. Note that, in order to keep the system finite, only r and s values for which both elongation factors g_p and g_m are smaller than 1 are possible. Hence, the point (r, s) must be inside the gray shaded area in Figure 3, which will be called the constrained monomer concentration region.

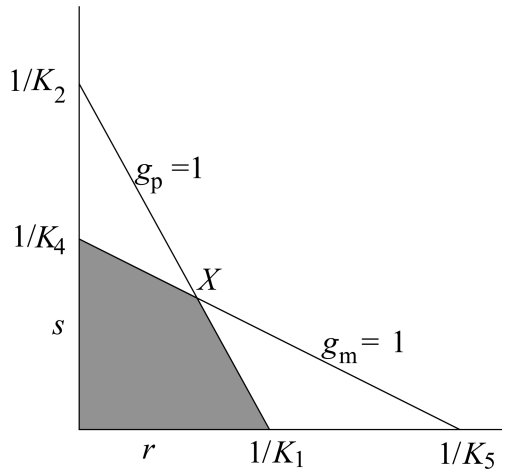

Figure 3. The (r, s) plane with the lines $g_p = 1$ and $g_m = 1$. The constrained monomer concentration region (gray shaded) for the free monomer concentrations is given by $g_p < 1$ and $g_m < 1$.

Computing the CD Effect. For given total concentrations r_{tot} and s_{tot}, the (free) monomer concentrations r and s can (in principle) be solved from eqs 28 and 29, but these monomer concentrations can, in most cases, not be measured experimentally. To be able to compare the results of our model with experimental data like, for example, circular dichroism (CD) measurements, the concentration of all monomers in P-type supramolecular polymers (p_{tot}) and the concentration of monomers in M-type supramolecular polymers (m_{tot}) are needed, as the measured CD intensity is assumed to be proportional to their difference

$$CD = N(p_{tot} - m_{tot})$$

where N is a constant with dimension mdeg/mol, denoting the CD effect per mol.

Using eqs 14 and 15, we obtain for the concentration of all R and S molecules in P-type aggregates

$$p_{tot} = r_P + s_P = \frac{\sigma_P}{K_1}\frac{g_p^2(2 - g_p)}{(1 - g_p)^2} \tag{30}$$

For the total monomer concentration in M-type aggregates we obtain using eqs 26 and 27 the expression

$$m_{tot} = s_M + r_M = \frac{\sigma_M}{K_4}\frac{g_m^2(2 - g_m)}{(1 - g_m)^2} \tag{31}$$

Because the elongation factors g_p and g_m depend only on the monomer concentrations r and s, the values of p_{tot} and m_{tot} can be computed once the monomer concentrations r and s are known.

3. PROPERTIES OF THE MASS-BALANCE EQUATIONS

In the previous section, we have derived the mass-balance system eqs 28 and 29 for the monomer concentrations r and s. A simple analytic solution to these two nonlinear equations seems not possible. First we discuss a numerical solution of the mass-balance equations, and in the subsequent subsections, we consider the form of titration curves and melting curves and the related phase diagram.

Numerical Solution of the Model Equations. The system eqs 28 and 29 can in principle be solved using a suitable numerical method. To get an impression of the contribution of the various terms in eq 28, we rewrite this equation as

$$1 + g_p(2 - g_p)\frac{\sigma_P}{(1 - g_p)^2} + \frac{K_5}{K_4}g_m(2 - g_m)\frac{\sigma_M}{(1 - g_m)^2} = \frac{r_{tot}}{r}$$

In the left-hand side, $g_p(2 - g_p) \leq 1$, $g_m(2 - g_m) \leq 1$ and, assuming R monomers have less affinity with M-type aggregates than S monomers, $K_5/K_4 < 1$. Furthermore, the cooperativity factors σ_P and σ_M are usually small. Hence, if the right-hand side is large, which is the interesting case, at least one of the denominators $(1 - g_p)^2$ or $(1 - g_m)^2$ must also be very small. This means the solution (r, s) of eqs 28 and 29 lies very close to the lines $g_p = 1$ and/or $g_m = 1$. In this region, the left-hand sides of the equations have very high gradients, which may be cumbersome for a numerical method. Therefore, we introduce new variables x and y as

$$x = \frac{1 - g_p}{\sqrt{\sigma_P}} \equiv \frac{1 - K_1 r - K_2 s}{\sqrt{\sigma_P}} \tag{32}$$

$$y = \frac{1 - g_m}{\sqrt{\sigma_M}} \equiv \frac{1 - K_4 s - K_5 r}{\sqrt{\sigma_M}} \tag{33}$$

The system eqs 28 and 29 can now, by elementary algebra, be rewritten in terms of the new unknowns x and y. In these new variables, the system can easily be solved by a suitable numerical method. We used the Matlab function *lsqnonlin* to

dx.doi.org/10.1021/jp300622m | J. Phys. Chem. B 2012, 116, 5291−5301

minimize the sum of the squared errors of the two resulting equations in x and y. From the solutions x and y, the free monomer concentrations r and s can be computed by solving eqs 32 and 33 for r and s. The total material in P-type aggregates p_{tot}, the total material in M-type aggregates m_{tot}, and the resulting CD effect can then be computed from eqs 30 and 31.

The above computation can be repeated for different values of the equilibrium constants (corresponding to different temperatures, leading to melting curves) or for different values of r_{tot} and s_{tot} (leading to titration curves). We first consider titration curves, where the total concentration $r_{tot} + s_{tot} = c_{tot}$ is constant and the relative excess of one of the two components will be described by the enantiomeric excess ee, defined as

$$ee = \frac{r_{tot} - s_{tot}}{c_{tot}} \tag{34}$$

A typical solution is shown in Figure 4. To describe the behavior of this solution, we divide the ee range into parts I, IIa, and IIb, as indicated in Figure 4. The solution shows an interesting behavior. First, there is a nonlinear increase of the CD effect as the enantiomeric excess ee increases. For (almost) all values of the enantiomeric excess between −1 and 1, the net helicity (i.e., $(p_{tot} - m_{tot})/(p_{tot} + m_{tot})$) differs from the enantiomeric excess ee, a phenomenon known as the majority-rules effect.[19] Second, for ee in region I, the free monomer concentrations r and s are almost constant. If the ee increases in region I, the total material in P-type aggregates p_{tot} grows apparently linearly (starting from 0), while the total material in the M-type aggregates m_{tot} decreases apparently linearly (until 0). Consequently, the CD effect, described by $p_{tot} - m_{tot}$, also increases linearly in region I. Third, in region IIa, no M-type aggregates are left, that is, $m_{tot} = 0$. Moreover, with increasing ee, the concentration of free R monomers (r) and the total material in P-type aggregates (p_{tot}) grows slightly, while the concentration of free S monomers (s) decreases until it reaches 0 at $ee = 1$. Similar effects occur in region IIb if ee decreases. We will use ee_{cr}^- and ee_{cr}^+ for the "critical ee values" at the border between regions IIb and I and regions I and IIa, respectively.

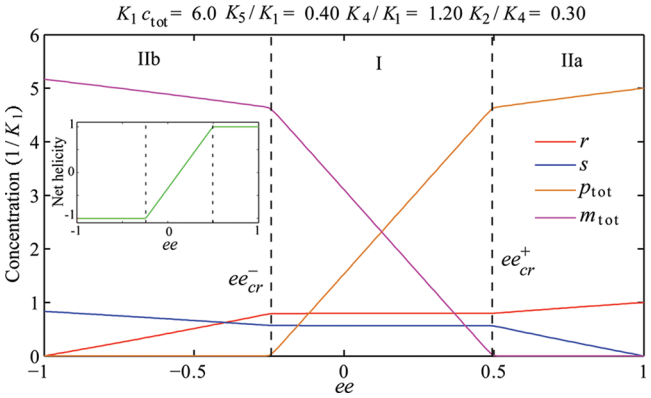

Figure 4. Typical speciation plot of a supramolecular copolymerization of two (nonenantiomerically related) monomer types. The monomer concentrations r and s and the total material in supramolecular polymers p_{tot} and m_{tot} as a function of ee. The two vertical lines indicate the position of ee_{cr}^- and ee_{cr}^+. The inset shows the net helicity, given by $(p_{tot} - m_{tot})/(p_{tot} + m_{tot})$.

Analyzing Titration Curves. It turns out that, in the case of high cooperativity and a sufficiently large total concentration, many of the remarkable properties of this system can be explained by a simple study of the mass-balance equations. Hence, in this subsection we assume that the cooperativity factors σ_P and σ_M are small and that the total concentration is large, that is, $K_1 c_{tot} > 1$. In this case, we can derive simple approximations for the various concentrations, as shown in Figure 4, and for the critical values ee_{cr}^- and ee_{cr}^+.

So far we have considered the general case, that is, the equilibrium constants K_1 and K_2 and cooperativity factor σ_P, for P-type aggregates can be different from the equilibrium constants K_4 and K_5 and cooperativity factor σ_M for the M-type aggregates. To avoid cumbersome formulas, we assume in the remaining part of this section that, unless otherwise stated, the role of R and S molecules in P-type supramolecular polymers is identical to the role of S and R molecules in M-type supramolecular polymers. This happens, for instance, if R and S are two enantiomers of the same molecule. In this symmetric situation, $K_4 = K_1$, $K_5 = K_2$, and $\sigma_M = \sigma_P = \sigma$. The results for the general nonsymmetric case are given in the Supporting Information, section SI-3.

The properties of titration curves can be found by examining the relation between the total concentrations r_{tot}, s_{tot} and the corresponding free monomer concentrations r, s. Because in a titration curve the sum of the total concentrations $r_{tot} + s_{tot}$ is constant, the point (r_{tot}, s_{tot}) lies on a straight line (the dashed line in Figure 5b).

Case 1, Small ee. First we consider situations with a small enantiomeric excess ee, that is, where the point (r_{tot}, s_{tot}) lies in region I in Figure 5. If $ee = 0$, the mass-balance equations for r and s are identical and P-type and M-type aggregates are

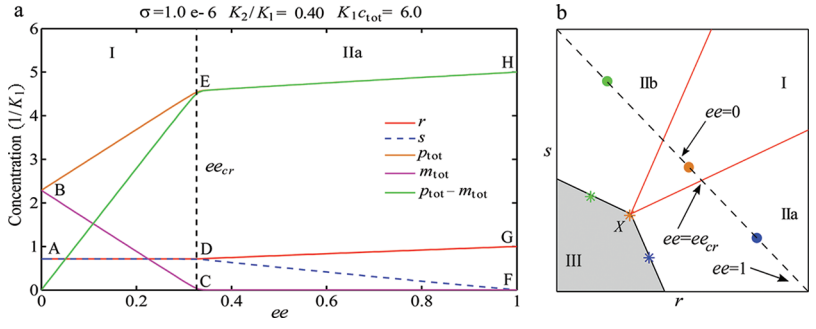

Figure 5. Typical speciation plot and phase diagram for the supramolecular copolymerization of two enantiomers, that is, $K_4 = K_1$, $K_5 = K_2$, and $\sigma_M = \sigma_P$. (a) Monomer concentrations r and s and total material in aggregates p_{tot} and m_{tot} as function of ee. (b) The situation in the r, s plane, with three points $(r_{tot}, s_{tot}$; blue, brown, and green circles), and the corresponding free monomer points (r, s; blue, brown, and green stars).

dx.doi.org/10.1021/jp300622m | J. Phys. Chem. B 2012, 116, 5291−5301

present in equal amounts. For *ee* values close to 0, still both P-type and M-type aggregates will be present in the system, although no longer in equal amounts. However, as long as both aggregate types are present, the corresponding elongation factors g_p and g_m must both be approximately 1, implying that the point (r, s) must be inside the constrained monomer concentration region, very close to the intersection point X. The brown points in Figure 5b are an example of this case. It is easily verified that the intersection point X, being the intersection of the two lines $g_p = K_1r + K_2s = 1$ and $g_M = K_1s + K_2r = 1$, has coordinates $r_X = s_X = 1/(K_1 + K_2)$. This explains why in Figure 5a the free monomer concentrations r and s are approximately constant for small values of *ee*. Moreover, the values of the free monomer concentrations in this region are approximately given by $r = s = 1/(K_1 + K_2)$. This corresponds to the line AD in Figure 5a.

The fact that r and s are approximately equal to $1/(K_1 + K_2)$ for small values of *ee* allows a simple solution of the mass-balance system eqs 28 and 29 in this case. Equations 30 and 31, the mass-balance equations, can be rewritten as

$$r + \frac{K_1 r}{g_p} p_{tot} + \frac{K_2 r}{g_m} m_{tot} = r_{tot} \tag{35}$$

$$s + \frac{K_2 s}{g_p} p_{tot} + \frac{K_1 s}{g_m} m_{tot} = s_{tot} \tag{36}$$

Substitution of $r = s = 1/(K_1 + K_2)$ in these equations yields

$$K_1 p_{tot} + K_2 m_{tot} = (K_1 + K_2) r_{tot} - 1$$

$$K_2 p_{tot} + K_1 m_{tot} = (K_1 + K_2) s_{tot} - 1$$

This is a system of two simple linear equations for p_{tot} and m_{tot}, with a solution (written in terms of *ee* instead of r_{tot} and s_{tot})

$$p_{tot} = \frac{c_{tot}}{2} - \frac{1}{K_1 + K_2} + ee\frac{c_{tot}}{2}\frac{K_1 + K_2}{K_1 - K_2} \tag{37}$$

$$m_{tot} = \frac{c_{tot}}{2} - \frac{1}{K_1 + K_2} - ee\frac{c_{tot}}{2}\frac{K_1 + K_2}{K_1 - K_2} \tag{38}$$

This result shows that in region I indeed p_{tot} increases linearly with *ee*, while m_{tot} decreases linearly with *ee*. Hence, the lines BC and BE in Figure 5a are straight lines. Because m_{tot} cannot become negative, the maximal *ee* value, for which this solution is possible, can be found by solving $m_{tot} = 0$. This gives the critical *ee* value

$$ee_{cr} = \frac{K_1 - K_2}{K_1 + K_2}\left(1 - \frac{2}{c_{tot}(K_1 + K_2)}\right) \tag{39}$$

The red lines in Figure 5b correspond to r_{tot} and s_{tot} values with an enantiomeric excess equal to the critical value ee_{cr} or $-ee_{cr}$ (see also Supporting Information, section SI-3). Hence, all points (r_{tot}, s_{tot}) in region I have an *ee* value with $|ee| < ee_{cr}$, and the behavior described above holds for all these points.

Case 2, Large ee. Next we consider situations with a large absolute value of the enantiomeric excess. More precisely, we study the case that the point (r_{tot}, s_{tot}) is either in region IIa, which means $ee > ee_{cr}$, or in region IIb, which means $ee < -ee_{cr}$. Because these two cases are completely symmetrical, we will only consider the first case. In this situation there are still P-type aggregates, so $g_p \approx 1$, but there are no M-type aggregates anymore, so g_m is not close to 1. This means the point (r, s) lies close to the line $g_p = 1$, but below the intersection point X, see the blue points in Figure 5b. Because $m_{tot} \approx 0$, we can now write the mass-balance equations eqs 35 and 36 by

$$r + \frac{K_1 r}{g_p} p_{tot} = r_{tot} \tag{40}$$

$$s + \frac{K_2 s}{g_p} p_{tot} = s_{tot} \tag{41}$$

The derivation of an approximate solution of the mass-balance equations is somewhat more complicated in this case. The details are given in the Supporting Information, section SI-2. The results are

$$r = \frac{-K_1 c_{tot} + \kappa - 1 + \sqrt{D}}{2K_1(\kappa - 1)} \tag{42}$$

$$s = \frac{K_1 c_{tot} + \kappa - 1 - \sqrt{D}}{2K_2(\kappa - 1)} \tag{43}$$

$$p_{tot} = \frac{1}{K_1}\left(\frac{(1 + ee)c_{tot}}{2r} - 1\right) \tag{44}$$

where

$$D = (K_1 c_{tot})^2 + 2ee K_1 c_{tot}(\kappa - 1) + (\kappa - 1)^2 \tag{45}$$

$$\text{and } \kappa = K_1/K_2$$

The expressions eqs 42–44 correspond to the lines DG, DF, and EH in Figure 5a, respectively. Note that, although Figure 5a suggests that these are straight lines, our computation shows that r, s, and p_{tot} are formally no linear functions of *ee*.

Finally, we use the given expressions to compute the various concentrations for $ee = 1$, corresponding to the situation in which no S molecules are present in the system. Substitution of $ee = 1$ in eq 45 gives $D = (K_1 c_{tot} + \kappa - 1)^2$. When used in eqs 42–44, this yields, for $ee = 1$, the values

$$r = \frac{1}{K_1}$$

$$s = 0$$

$$p_{tot} = c_{tot} - \frac{1}{K_1}$$

These three concentrations correspond to the points G, F, and H in Figure 5a, respectively. Note that $ee = 1$ corresponds to a one-component system and the monomer concentration $r = 1/K_1$ is equal to the limiting monomer concentration in the nucleation–elongation model, see, for instance, Zhao and Moore.[7] Recall that the analytical approximations given here are derived under the assumption of a small cooperativity factor σ and a sufficiently large total concentration c_{tot}. For these situations, the formulas derived agree very well with the numerically computed solution. For instance, for the case of Figure 5 or the symmetric supramolecular copolymerization example in section 4, the differences between the numerically found solutions of the mass-balance equations and the approximations given here are hardly visible.

Analyzing Melting Curves. In a melting experiment we consider a system with total concentrations r_{tot} and s_{tot} fixed, while the temperature is varied. To compute the equilibrium

dx.doi.org/10.1021/jp300622m | J. Phys. Chem. B 2012, 116, 5291–5301

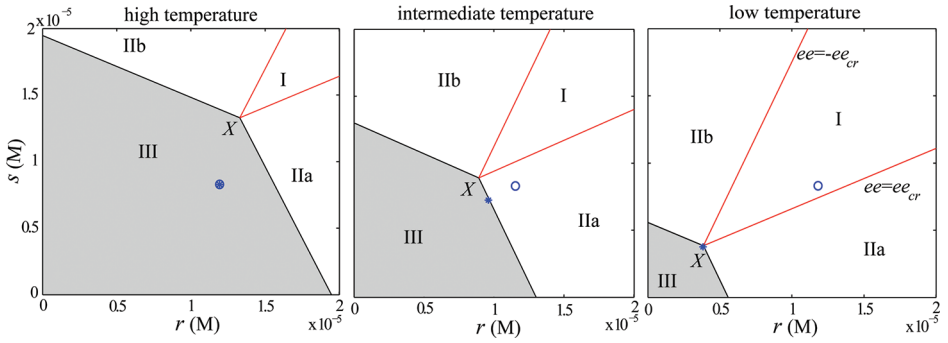

Figure 6. Phase diagram for three typical temperatures with the constrained monomer concentration region (III) in gray. The red lines indicate the points with an *ee* value equal to $\pm ee_{cr}$ for that temperature. The open blue circle is the (fixed) point (r_{tot}, s_{tot}) and the blue star is the corresponding monomer concentration point (r, s) for three different temperatures.

state for varying temperatures, the dependence of the equilibrium constants on the temperature is needed. The equilibrium constant K of a reversible reaction is related to the change in standard Gibbs free energy ΔG^0 by $K = e^{-\Delta G^0/(RT)}$, where the standard Gibbs free energy change ΔG^0 consists of an enthalpy term ΔH^0 as well as an entropy term $T\Delta S^0$. The parameters K_1, K_2, and σ are therefore expressed in terms of an enthalpy of elongation ΔH^0, an entropy of elongation ΔS^0, a nucleation penalty ΔH^0_{nucl}, and a mismatch penalty ΔH^0_{mm}, according to

$$K_1 = e^{-(\Delta H^0 - T\Delta S^0)/(RT)} \tag{46}$$

$$K_2 = K_1 e^{\Delta H^0_{mm}/(RT)} \tag{47}$$

$$\sigma = \frac{\hat{K}_1}{K_1} = \frac{\hat{K}_2}{K_2} = e^{\Delta H^0_{nucl}/(RT)} \tag{48}$$

Similar to the previous subsection, we assume that the cooperativity factor σ is small in the considered temperature range. Because the equilibrium constants depend on the temperature, also the constrained monomer concentration region (see Figure 3) for the free monomer concentrations is temperature-dependent. Figure 6 shows the typical situation for three temperatures regimes. In all three cases, the open blue circle is the fixed point (r_{tot}, s_{tot}), with an enantiomeric excess $ee = 0.18$, and the blue star is the corresponding monomer concentration point (r, s) for that temperature.

Case 1, High T. When the temperature is high (Figure 6, left), the equilibrium constant K_1 and K_2 have small values, hence, the constrained monomer concentration region is large. The (fixed) point (r_{tot}, s_{tot}) lies well inside region III, which is identical to the constrained monomer concentration region. P-type and M-type aggregates are formed if the monomer concentration point (r, s) is very close to the lines $g_p = K_1 r + K_2 s = 1$ and $g_m = K_1 s + K_2 r = 1$, respectively. Because $r \leq r_{tot}$ and $s \leq s_{tot}$, that is not possible in this case. Hence, the concentration of aggregates will be very low and the free monomer concentrations are (almost) equal to the total concentrations, that is, $r = r_{tot}$ and $s = s_{tot}$. Consequently, in Figure 6, left, the open circle and the star coincide.

Case 2, Intermediate T. If the system is cooled down (Figure 6, middle), the equilibrium constants K_1 and K_2 become larger and the constrained monomer concentration region becomes smaller. The point (r_{tot}, s_{tot}) now lies in region IIa and, hence, the *ee* value is larger than the critical value ee_{cr} at that temperature. Consequently, only P-type aggregates will be formed. The growth of P-type aggregates will be initiated if the temperature has reached the value where the point (r_{tot}, s_{tot}) passes the line $g_p = 1$, which forms the border between regions III and IIa. Consequently, the elongation temperature T_e^p of P-type supramolecular polymers is defined as the temperature such that

$$K_1 r_{tot} + K_2 s_{tot} = 1 \tag{49}$$

where the dependence of K_1 and K_2 on the temperature is given by eqs 46 and 47.

Case 3, Low T. If the temperature is decreased further, the constrained monomer concentration region becomes smaller, and at a certain temperature, the point (r_{tot}, s_{tot}) enters region I, see Figure 6, right. Because the intersection point X moves to the origin and the angle between the two red lines goes to 90°, this will eventually always happen. Now the absolute value of the *ee* is smaller than the critical value ee_{cr} at that temperature, and both P- and M-type aggregates will be present. The growth of M-type aggregates will be initiated if the temperature has reached the value where the point (r_{tot}, s_{tot}) passes the line between regions IIa and I. This line is defined by $ee = ee_{cr}$, see Figure 5b. Using eqs 34 and 39, this equation can be written as

$$K_1 s_{tot} - K_2 r_{tot} = \frac{K_1 - K_2}{K_1 + K_2} \tag{50}$$

The elongation temperature T_e^M of M-type supramolecular polymers is defined as the temperature such that this equation holds.

The typical temperature-dependent behavior of the various concentrations in a melting curve is shown in Figure 7a. Above T_e^p, there are no supramolecular polymers, and the free monomer concentrations are equal to the total concentrations. If the temperature comes below T_e^p, P-type aggregates are formed, but the concentration of M-type aggregates is zero. The CD effect, being proportional to $p_{tot} - m_{tot}$, grows strongly with decreasing temperature. If the temperature falls below T_e^M growth of M-type aggregates is initiated. Because the M-type aggregates grow faster than P-type aggregates as the temperature decreases, the difference $p_{tot} - m_{tot}$ decreases slowly with decreasing temperature. Unfortunately, simple expressions for both elongation temperatures T_e^p and T_e^M cannot be given, except in the limiting cases $ee = 0$ and 1. However, the equations for T_e^p and T_e^M can easily be solved numerically. In Figure 7b, an example of the dependence of the elongation temperatures on the enantiomeric excess *ee* is shown.

dx.doi.org/10.1021/jp300622m | J. Phys. Chem. B 2012, 116, 5291−5301

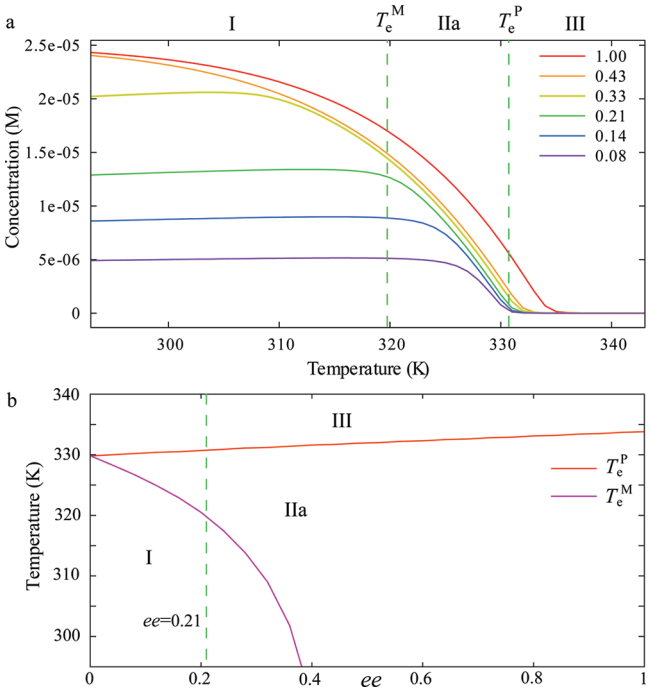

Figure 7. Model results for supramolecular copolymerization of (*R*)-**1** and (*S*)-**1**. (a) Difference $p_{tot} - m_{tot}$ (proportional to the CD effect) as function of the temperature for different *ee* values and a total concentration $c_{tot} = 2.5 \times 10^{-5}$ M; the green lines indicate the elongation temperatures at *ee* = 0.21. (b) Corresponding elongation temperatures T_e^P and T_e^M as function of the *ee*.

A particular simple formula can be given for the difference $p_{tot} - m_{tot}$ in region I, namely

$$p_{tot} - m_{tot} = \frac{ee\ c_{tot}}{\tanh(-\Delta H^0_{mm}/(2RT))}$$

This formula shows that the CD effect indeed slightly decreases when cooling down the system in region I. A detailed derivation is given in the Supporting Information, section SI-4.

4. COMPARISON TO EXPERIMENTAL DATA

Next, we will compare results of the model with various experimental data. In all cases, the parameters K_1, K_2, and σ are expressed in terms of an enthalpy of elongation ΔH^0, an entropy of elongation ΔS^0, a nucleation penalty ΔH^0_{nucl} and a mismatch penalty ΔH^0_{mm}.

Symmetric Supramolecular Copolymerization. In ref 21, we have compared the results of a similar model with experimental data for the case of supramolecular copolymerization of benzene-1,3,5-tricarboxamides (BTAs).[17,25] Fitting of experimental data[17,25] to our model yields the parameter values $\Delta H^0 = -71.9$ kJ/mol, $\Delta S^0 = -0.1273$ kJ/mol/K, $\Delta H^0_{nucl} = -27.4$ kJ/mol and $\Delta H^0_{mm} = -2.1$ kJ/mol. Similar to ref 21, the titration curves and melting curves predicted by the current model with these parameters show a very good agreement with the experimentally found curves, see also section SI-5 of the Supporting Information. Note that the current model, in contrast to the model in ref 21, allows two-sided growth of the supramolecular polymers. To explain the phase regions we show in Figure 7a, the computed melting curves, that is, the computed values of $p_{tot} - m_{tot}$ as a function of the temperature for mixtures with *ee* values from 0.08 to 1.0. The two vertical green lines in Figure 7a give the positions of the elongation temperatures T_e^P and T_e^M for the case *ee* = 0.21. If the temperature decreases below T_e^P P-type aggregates are formed, which leads to an increasing value of $p_{tot} - m_{tot}$. If after further cooling the temperature T_e^M is reached, also M-type aggregates are formed. The net effect is that $p_{tot} - m_{tot}$ decreases. Figure 7b gives the computed elongation temperatures T_e^P and T_e^M for $c_{tot} = 2.5 \times 10^{-5}$ M.

Nonsymmetric Supramolecular Copolymerization. So far we only considered the symmetric case where the mismatch penalty for a R monomer in an M-type aggregate is equal to the mismatch penalty for an S monomer in a P-type aggregate, as expected for two enantiomers. However, majority-rules titrations can also be performed with molecules that are not enatiomerically related. For example, Smulders et al.[25] report on mixed majority-rules experiments on different combinations of symmetrically and asymmetrically substituted benzene-1,3,5-tricarboxamides, as shown in Figure 1, in which two monomers with opposite chirality and different numbers of stereogenic centers were mixed. By choosing the elongation enthalpies and entropies for supramolecular polymers with the preferred helicity equal, that is, $K_4 = K_1$, we only need a second mismatch penalty. Instead of the single mismatch penalty sofar, we will thus use two mismatch penalties; $\Delta H^0_{mm,P}$ for a S monomer in a P-type supramolecular polymer and $\Delta H^0_{mm,M}$ for a R monomer in a M-type supramolecular polymer, that is,

$$K_2 = K_1 e^{\Delta H^0_{mm,P}/(RT)}$$

$$K_5 = K_1 e^{\Delta H^0_{mm,M}/(RT)}$$

Figure 8 (case a) shows both the experimental data[25] as well as the model results for mixed majority-rules titrations using

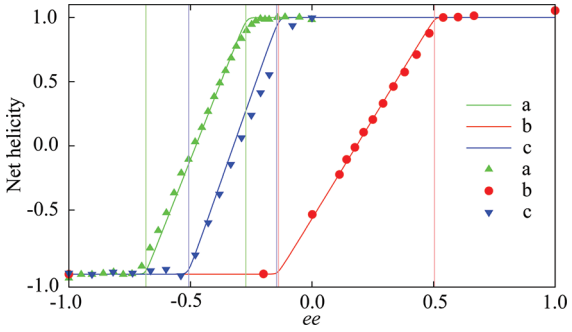

Figure 8. Comparison of experimental[25] (symbols) and calculated (lines) net helicity of mixed majority-rules (*R*)-**1**/(*S*)-**3** (a), (*S*)-**1**/(*R*)-**2** (b), and (*R*)-**2**/(*S*)-**3** (c). Temperature *T* = 293 K and total concentration $c_{tot} = 3.0 \times 10^{-5}$ M. The colored vertical lines indicate the critical values ee^-_{cr} and ee^+_{cr}.

monomers (*R*)-**1**, having three stereocenters, and (*S*)-**3**, having only a single stereocenter (see Figure 1). The mismatch penalties used in the model correspond to −0.7 kJ/mol per stereocenter, that is, one-third of the originally found −2.1 kJ/mol for the monomer having three stereocenters. Thus, $\Delta H^0_{mm,P} = -0.7$ kJ/mol and $\Delta H^0_{mm,M} = -2.1$ kJ/mol.

Figure 8 (case b) shows the experimental data[25] as well as the model results, but now for mixing (*S*)-**1** with (*R*)-**2**, respectively. Because (*S*)-**1** has three stereocenters and (*R*)-**2** has two stereocenters, the mismatch penalties are $\Delta H^0_{mm,P} = -2.1$ kJ/mol and $\Delta H^0_{mm,M} = -1.4$ kJ/mol.

In Figure 8 (case c), the experimental data[25] as well as the model results, for mixing (*R*)-**2** with (*S*)-**3** are shown.

dx.doi.org/10.1021/jp300622m | J. Phys. Chem. B 2012, 116, 5291−5301

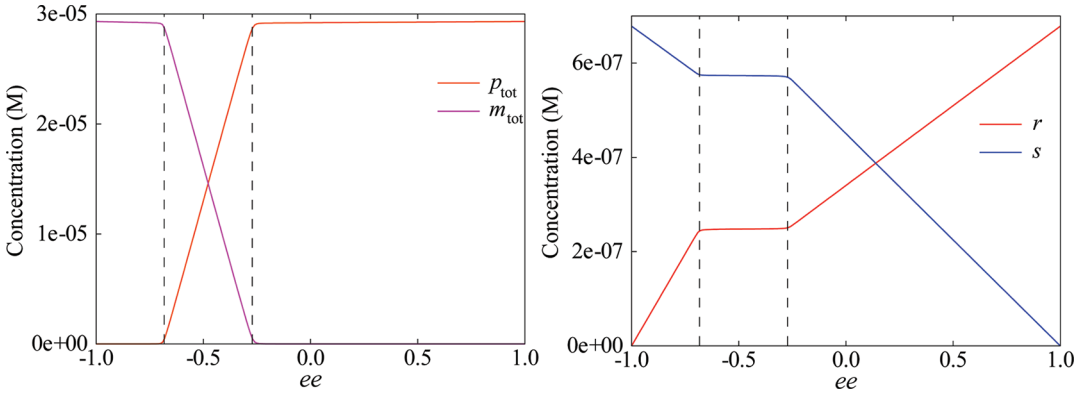

Figure 9. Calculated total material in P-type (p_{tot}) and M-type (m_{tot}) aggregates (left) and free monomer concentration (r and s, right) as a function of *ee* for majority-rules titrations in which (*R*)-**1** and (*S*)-**3** are varied. Temperature T = 293 K and total concentration $c_{tot} = 3.0 \times 10^{-5}$ M. The dashed vertical lines indicate the critical values ee_{cr}^{-} and ee_{cr}^{+}.

The mismatch penalties in this case are $\Delta H^0_{mm,P} = -0.7$ kJ/mol and $\Delta H^0_{mm,M} = -1.4$ kJ/mol. Also, in these mixed majority-rules experiments, the model results agree well again with the experimental data.

Figure 9 shows the individual concentrations for the (*R*)-**1**/(*S*)-**3** mixture corresponding to case a. The left part of the figure gives the total material in P- and M-type aggregates; in the right part, the free monomer concentrations are shown. Going from pure (*S*)-**3** (i.e., *ee* = −1.0) to pure (*R*)-**1** (i.e., *ee* = 1.0), the monomer concentration r increases and s decreases, except for the *ee*-range between ee_{cr}^{-} and ee_{cr}^{+}, where the net helicity changes from −1 to 1 and the monomer concentrations remain almost constant.

Isodesmic Supramolecular Copolymerization. Finally, we compare the results of our model with experimental data of an isodesmic supramolecular polymerization. We consider the C3-symmetrical disk-shaped compound (*S*)-**4** and (*R*)-**4** (Figure 2). It is shown by van Gestel et al.[20] that enantiomeric mixtures of these compounds display the majority-rules effect. Fitting of melting curves of the enantiomerically pure compounds yields the parameters $\Delta H^0 = -100.5$ kJ/mol, $\Delta S^0 = -0.2204$ kJ/mol/K, and $\Delta H^0_{nucl} = -0.06$ kJ/mol (see the section SI-6 of Supporting Information for more details). As expected for an isodesmic system, the nucleation penalty ΔH^0_{nucl} is almost zero.

In Figure 10 (green triangles), the results of a titration experiment[20] for a concentration $c_{tot} = 2.49 \times 10^{-5}$ M and a temperature T = 293 K are given. Here, the enantiomeric excess is defined as $ee = (s_{tot} - r_{tot})/c_{tot}$. The only remaining parameter to model these data is the mismatch penalty ΔH^0_{mm}. This mismatch penalty can in principle be obtained from the value of ee_{cr} (the kink in the CD data) or by fitting the computed titration curve with the experimental data. In the isodesmic case the clear separation of the *ee* range in different phase regions does not hold anymore, which makes it difficult to determine ee_{cr} from experimental data. We can, however, still fit the results of the model, that is, the numerical solution of the mass-balance equations, with the experimental data. That leads to a mismatch penalty ΔH^0_{mm} of −1.4 kJ/mol. The results are shown in Figure 10. Once again our model gives a very good description of the majority-rules effect. As expected for an isodesmic growth mechanism, the system behaves more smoothly; the strong separation between the phase regions of the cooperative case is absent. Note that computing the critical value of the enantiomeric excess with eq 39 leads to $ee_{cr} = 0.274$, which indeed corresponds with the (vague) kink points in the curves for p_{tot} and m_{tot} in Figure 10.

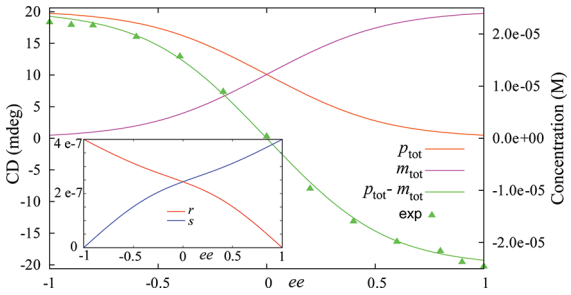

Figure 10. Comparison of experimental[20] CD data (left axis) and model results (p_{tot}, m_{tot}, and $p_{tot} - m_{tot}$, right axis) of the supramolecular copolymerization of (*S*)-**4** and (*R*)-**4** for $c_{tot} = 2.49 \times 10^{-5}$ M and T = 293 K. The inset shows the corresponding free monomer concentrations r and s.

5. DISCUSSION AND CONCLUSION

We have introduced an equilibrium model to describe chiral amplification in cooperative and isodesmic supramolecular copolymerization. In contrast to our previous efforts,[21] it describes two-sided growth of the aggregates and also allows for nonenantiomerically related monomers. Our model provides the equilibrium state for a supramolecular copolymerization, where each added molecule can independently be one of two type monomers (R or S) and each supramolecular polymer can be formed with one out of two helicities (P or M). The concentrations of the free monomers r and s in equilibrium are obtained as the solution of the mass-balance equations. Two methods are described to solve the mass balance equations. Besides a numerical method, analytical formulas are derived that give very good approximations to the various concentrations for cooperative supramolecular copolymerizations.

From the solutions of the mass-balance equations, that is, the free monomer concentrations r and s, the total material in P- and M-type supramolecular polymers is computed. Assuming the difference between the total material in P- and M-type aggregates is proportional to the CD effect, the model results are compared to experimental data. The model gives a very good description of experimental titration and melting curves, also for nonsymmetric supramolecular copolymerization. Moreover, a single parameter (the mismatch penalty ΔH^0_{mm}) suffices to describe the interaction between R and S molecules.

dx.doi.org/10.1021/jp300622m | J. Phys. Chem. B 2012, 116, 5291−5301

The value of ΔH^0_{mm} depends only on the used types of R and S molecules and not on the temperature. In particular, no so-called helix reversals,[18] as used by Smulders et al.,[25] are needed.

Although our model is based on monomer addition, other or additional reactions can be used. For instance, breaking of P-type supramolecular polymers or the formation of a P-type supramolecular polymer by coupling two shorter P-type supramolecular polymers are not possible in the current system of reactions but can easily be added. In fact, the principle of detailed balance allows to compute the equilibrium constants of additional reactions of this type. An example is given in the Supporting Information, section SI-7.

The model also yields a phase diagram, that is, each point (r_{tot}, s_{tot}, T) is either type I (monomers and P- and M-type aggregates), type IIa (monomers and P-type aggregates), type IIb (monomers and M-type aggregates), or type III (only monomers). The boundaries between the various regions are explicitly given. For instance, for a fixed temperature T the boundary between region I and region IIa is the line $ee = ee_{cr}$ (see Figure 5b), while for fixed concentrations r_{tot} and s_{tot}, this boundary is at temperature T_e^M (see Figure 7). An explicit formula for the critical ee has been given. The elongation temperatures for P- and M-type supramolecular polymers T_e^P and T_e^M are defined as solutions of one-variable equations and can be computed numerically. These type of results are a consequence of the description of the equilibrium state as the solution of a system of mathematical equations and cannot be obtained by simulations.[21]

The advantage of the model is also that it yields all individual concentrations (see, for instance, Figure 9), which gives new insight in titration curves as well as melting curves for mixed systems. With different choices of the rate constants, similar models can be used to describe other nonlinear phenomena, such as the sergeants-and-soldiers effect.[26] The model can also be extended to more complex molecular systems, for example, containing more different components, like the diluted majority-rules principle. A similar approach is also possible if the nucleus size n is larger than 2.

■ ASSOCIATED CONTENT

Ⓢ Supporting Information

Details of several computations, results for the nonsymmetric case, parameter fits for the experimental data of the examples, and software for fitting model parameters. This material is available free of charge via the Internet at http://pubs.acs.org.

■ AUTHOR INFORMATION

Corresponding Author

*E-mail: h.m.m.t.eikelder@tue.nl.

Notes

The authors declare no competing financial interest.

■ ACKNOWLEDGMENTS

We thank Bert Meijer for drawing our attention to this problem, Anja Palmans for the many stimulating discussions and the provision of experimental data, Charley Schaefer for his help with the fitting software, and Koen Pieterse for the art work.

■ REFERENCES

(1) de Greef, T. F. A.; Smulders, M. M. J.; Wolffs, M.; Schenning, A. P. H. J.; Sijbesma, R. P.; Meijer, E. W. *Chem. Rev.* **2009**, *109*, 5687−5754.

(2) Wu, J.; Fechtenkötter, A.; Gauss, J.; Watson, M. D.; Kastler, M.; Fechtenkötter, C.; Wagner, M.; Müllen, K. *J. Am. Chem. Soc.* **2004**, *126*, 11311−21.

(3) Chen, Z.; Lohr, A.; Saha-Möller, C.; Würthner, F. *Chem. Soc. Rev.* **2009**, *38*, 564−584.

(4) Xue, W.-F.; Homans, S. W.; Radford, S. E. *Proc. Natl. Acad. Sci. U.S.A.* **2008**, *105*, 8926−8931.

(5) Martin, R. *Chem. Rev.* **1996**, *96*, 3043−3064.

(6) Goldstein, R.; Stryer, L. *Biophys. J.* **1986**, *50*, 583−599.

(7) Zhao, D.; Moore, J. S. *Org. Biomol. Chem.* **2003**, *1*, 3471−3491.

(8) Jonkheijm, P.; van der Schoot, P.; Schenning, A. P. H. J.; Meijer, E. W. *Science* **2006**, *313*, 80−83.

(9) Douglas, J. F.; Dudowicz, J.; Freed, K. F. *J. Chem. Phys.* **2008**, *128*, 224901.

(10) Hunter, C. A.; Anderson, H. L. *Angew. Chem., Int. Ed.* **2009**, *48*, 7488−7499.

(11) Ercolani, G.; Schiaffino, L. *Angew. Chem., Int. Ed.* **2011**, *50*, 1762−1768.

(12) Oosawa, F.; Kasai, M. *J. Mol. Biol.* **1962**, *4*, 10−21.

(13) Frieden, C.; Goddette, D. W. *Biochemistry* **1983**, *22*, 5836−5843.

(14) Powers, E. T.; Powers, D. L. *Biophys. J.* **2006**, *91*, 122−132.

(15) Morris, A. M.; Watzky, M. A.; Finke, R. G. *Biochim. Biophys. Acta* **2009**, *1794*, 375−397.

(16) Smulders, M. M. J.; Schenning, A. P. H. J.; Meijer, E. W. *J. Am. Chem. Soc.* **2008**, *130*, 606−611.

(17) Smulders, M. M. J.; Filot, I. A. W.; Leenders, J. M. A.; van der Schoot, P.; Palmans, A. R. A.; Schenning, A. P. H. J.; Meijer, E. W. *J. Am. Chem. Soc.* **2010**, *132*, 611−619.

(18) van Gestel, J. *Macromolecules* **2004**, *36*, 3894−3898.

(19) Green, M. M.; Peterson, N. C.; Sato, T.; Teramoto, A.; Cook, R.; Lifson, S. A. *Science* **1995**, *268*, 1860−1866.

(20) van Gestel, J.; Palmans, A. R. A.; Titulaer, B.; Vekemans, J. A. J. M.; Meijer, E. W. *J. Am. Chem. Soc.* **2005**, *127*, 5490−5494.

(21) Markvoort, A. J.; ten Eikelder, H. M. M.; Hilbers, P. A. J.; de Greef, T. F. A.; Meijer, E. W. *Nat. Commun.* **2011**, *2*, 509.

(22) Alberty, R. A. *J. Chem. Educ.* **2004**, *81*, 1206−1209.

(23) Onsager, L. *Phys. Rev.* **1931**, *37*, 405−426.

(24) Wegscheider, R. *Z. Phys. Chem.* **1902**, *39*, 257−303.

(25) Smulders, M. M. J.; Stals, P. J. M.; Mes, T.; Paffen, T. F. E.; Schenning, A. P. H. J.; Palmans, A. R. A.; Meijer, E. W. *J. Am. Chem. Soc.* **2010**, *132*, 620−626.

(26) Green, M. M.; Reidy, M. P. *J. Am. Chem. Soc.* **1989**, *111*, 6452−6454.